ORIGINAL CONTRIBUTION

EXPERIMENTAL ONCOLOGY

https://doi.org/10.15407/exp-oncology.2025.02.167

Maham Ansari, Rafiullah Rafiullah, Abdul Wali, Afrasiab Khan Tareen, Imrana Niaz Sultan, Muhammad Mushtaq Yasinzai *

Department of Biotechnology, Faculty of Life Sciences and Informatics, Balochistan University of Information Technology, Engineering and Management Sciences (BUITEMS), Quetta, Pakistan

* Correspondence: Email: muhammad.mushtaq1@buitms.edu.pk

IDENTIFICATION AND FUNCTIONAL CHARACTERIZATION OF MICRORNAS REGULATING HTERT

Background. Telomerase is a ribonucleoprotein (RNP) reverse transcriptase that replicates the ends of chromosomes, thereby maintaining genome integrity, and its inhibition may be envisioned to prevent carcinogenesis or treat cancer patients. Various approaches have been used to target hTERT, and one of the promising strategies is the use of hTERT-targeting microRNAs (miRNAs). **Aim.** To investigate the interaction of miRNAs with hTERT, describing the strength, affinity, preferred binding orientation, and in vitro verification of miRNA on hTERT expression in cancer. **Materials and Methods.** The miRWalk, TargetScan, and miRDB databases were used for screening. Consistently, five top-hit miRNAs were found in all three databases that could interact with hTERT mRNA, namely, *hsa-miR-4651, hsa-miR-608, hsa-miR-6796-5p, hsa-miR-6752-5p,* and *hsa-miR-6791-5p*. We applied stringent in silico tools to firstly model the structures of lead miRNA and hTERT mRNA. Then docking was performed, and finally stability of miRNA-mRNA complexes was analyzed using MD simulations. **Results.** The expression of the selected miRNAs was inhibited in the MCF-7 breast cancer cell line. The inhibition of *hsa-miR-6796-5p* was enhanced, while *hsa-miR-4651* significantly reduced the expression of hTERT protein. Moreover, the inhibition of *hsa-miR-4651* expression led to a reduction in melanoma and breast cancer cell proliferation. **Conclusion.** The current study provided a detailed procedure for identifying and verifying miRNAs against mRNAs, as well as highlighting the differential regulation of hTERT by specific miRNAs. It demonstrated that miRNA inhibition can modulate hTERT expression and cell proliferation, with potential implications for targeted cancer therapies. The strategy used in this study could also be applied to other genes for screening potential miRNAs.

Keywords: microRNA, hTERT, cancer, hsa-miR-6796-5p, hsa-miR-4651, binding orientation, affinity, cell proliferation.

Telomerase is a ribonucleoprotein (RNP) reverse transcriptase [1] that replicates the end of chromosomes and plays a vital role in maintaining genome integrity [1, 2]. Human telomerase is a holoenzyme containing two subunits. The human telomerase RNA component (hTR/hTERC) is encoded by the *TERC* gene, located on chromosome region 3q26, whereas the catalytically active pro-

Citation: Ansari Maham, Rafiullah Rafiullah, Wali Abdul, Tareen Afrasiab Khan, Sultan Imrana Niaz, Yasinzai Muhammad Mushtaq. Identification and functional characterization of microRNAs regulating hTERT. *Exp Oncol.* 2025; 47(2): 167-180. https://doi.org/10.15407/exp-oncology.2025.02.167

tein subunit of human telomerase reverse transcriptase (hTERT) is encoded by the *TERT* gene located at locus 5p13.33 [3—5].

Normal somatic cells lack telomerase activity and lose proliferative potency over time. This feature can be envisioned to prevent cancer. The inhibition of the telomerase activity would shorten telomere length by inducing cell senescence in the rapidly dividing cancer cells and, therefore, can effectively control the growth of the tumor [6]. The different approaches have been used to target hTERT, ranging from immunotherapies [7], which recognize tumor-associated antigens [8], to oligonucleotides, which directly bind to the telomere's end and prevent its extension [9], or small molecule inhibitors like BIBR1532 [10]. Another indirect approach is a G-quadruplex stabilization [11, 12], which disrupts the h*TERT* gene expression by inducing nucleoside analogs [13, 14].

There are many challenges in targeting hTERT, such as the unavailability of a high-resolution human telomerase structure, preclinical model limitations, and adaptive drug resistance, which makes hTERT targeting difficult. Furthermore, hTERT targeting therapies require treatment with a relevant agent for a long time before the anticancer effect can be analyzed. Due to reliance on gradual attrition of telomeres with each cell division, the cells may grow out as resistant to the drug, consequently making this strategy unsuitable for the first-line therapy. Another challenge is its expression in precursor cells like hematopoietic cells and stem cells, which are also affected by such therapies. Nevertheless, telomerase has remained an important target for anticancer therapy owing to its specificity to cancer cells and universality [15].

Considering these challenges in directly targeting telomerase, alternative approaches, particularly the use of miRNAs, have gained attention to regulate hTERT expression. miRNAs are small, non-coding RNA (approximately 22 nucleotides in length) that regulate several vital biological processes [16] like cell proliferation, differentiation, apoptosis, and migration [17]. miRNAs contribute to cancer development [18, 19] by acting as oncomiRs or tumor suppressors (TS) [18, 20]. OncomiRs are overexpressed in cancer cells and promote tumor growth by binding and suppressing mRNAs of tumor suppressor genes, whereas the tumor suppressor miRNA inhibits the expression of oncogene mRNA, and are usually underexpressed in cancer [21].

Likewise, *hTERT*-targeting-miRNAs negatively regulate h*TERT* expression, preventing tumorigenesis. These miRNAs are commonly downregulated in many cancers [22, 23]. The biology and functional studies of h*TERT*-targeting miRNAs have been thoroughly explored through a model based on in vivo studies [24—26]. miRNAs regulate hTERT expression in direct or indirect manners. Some miRNAs directly bind to the 3′ UTR region of hTERT or may hinder the hTERT protein production [27, 28]. Repressing the hTERT activity has been considered as an important approach to the anticancer therapy development [22, 29—33]. However, efforts made so far have led to inadequate clinical outcomes with the inability to inhibit hTERT expression or activity. Furthermore, such previous attempts of targeting hTERT have shown long-term cytotoxicity for the normal stem cells and their self-renewal capacity.

The aim of this research is to find miRNAs that can suppress *hTERT* expression and inhibit proliferation of rapidly dividing cancer cells. The current study explores the interaction of miRNAs and *hTERT*, describes the strength, affinity, preferred binding orientation, and interaction regions. The miRNAs that bind to the *hTERT* identified here could be valuable in identifying potential targeted therapies for silencing *hTERT*, thus preventing cancer progression.

Materials and Methods

miRNA binding site prediction on hTERT mRNA. The interaction and binding site of the miRNA on *hTERT* were analyzed using three databases. miRWalk (http://mirwalk.umm.uni-heidelberg.de) [34] integrates the experimentally verified data available for miRNA binding site prediction [34]. TargetScan (v8.0) (https://www.targetscan.org/vert_80/) [35, 36] identifies the conserved binding sites of MIRNAS using the seed region matching approach. miRDB (v6.0) (https://mirdb.org/) [37] uses the high throughput sequencing data to predict the miRNA-target interactions [36, 37].

miRNAs exhibiting strong and stable interactions with *hTERT* were selected based on binding energy threshold of ≤–30 kcal/mol, signifying high affinity interactions. Furthermore, only

miRNAs with a probability of 1 and an AU content of <0.6 were selected, indicating a stable binding site (AU-rich elements of the transcript with 30 nucleotides upstream and downstream of the predicted site) [38]. The common miRNA-*hTERT* interactions in three databases were considered for the miRNA-mRNA alignment.

Alignment between shortlisted miRNAs and mRNA. The RNA22 (v2.0) software (https://cm.jefferson.edu/rna22/Interactive/) [39] was employed to align the shortlisted miRNA against *hTERT* mRNA. The RNA22 uses a pattern-based approach and estimates the folding energy to predict the miRNA putative target site. It also predicts the miRNA that likely binds to the targeted site [40]. The seed size was kept at 7, with one unmatched base allowed in the seed region, specificity 61% and sensitivity 63%. The G:U wobble was not limited to the seed region. The maximum folding energy was kept at –12 kcal/ mol [41]. Nucleotide sequence of the *hTERT* was extracted from the National Center for Biotechnology Information (NCBI) [42], accession number NM_001193376.3. The miRbase database (v22; http://www.mirbase.org/) [43] was used to retrieve the sequences of the shortlisted miRNA. The sequence of *hTERT* RNA, along with the shortlisted miRNAs, was provided in the RNA 22 server. The alignment threshold of p-value <0.05 was considered significant [43].

Three-dimensional structure prediction of hTERT mRNA. For the prediction of the 3D model, the mRNA sequences that showed maximum interactions with the shortlisted miRNA were supplied to RNAComposer (v1.0) (https://rna composer.cs.put.poznan.pl/) [44]. The RNA Composer is a manually curated database that predicts tertiary and three-dimensional structures. The software takes 500 nucleotides as input; therefore, the regions greater than 500 nucleotides were trimmed into two regions for modeling. The method of CONTRAfold was selected for the prediction of secondary structures [45].

3D structure prediction of shortlisted miRNAs. The MC Fold (https://www.major.iric.ca/ MC-Fold/) [46] was used to predict the 3D structure of the shortlisted miRNA. The sequences of the miRNAs that showed maximum interactions with the shortlisted regions were used as input. The input RNA structure is decomposed into loops before predicting multiple secondary structures [46]. From the output files, the secondary structure with the minimum energy is submitted to MC Sym (https://www.major.iric.ca/MC-Sym/) [46] for the prediction of a stable tertiary structure. MC Sym generates structures by examining the RNA conformational search space [47].

Molecular docking between shortlisted miRNAs and hTERT. To identify the complexes of the shortlisted miRNA and the mRNA with the lowest binding affinity and optimized conformation, the HDOCK (v2021; http://hdock.phys.hust.edu.cn) [48] software was used. HDOCK uses the ab initio and template-based docking approach. The 3D structures of miRNA and mRNA are used as input, and the docking is run on default parameters. The 10 output results are generated for each input. A complex with the maximum confidence score >0.7 and with the least binding energy showed a strong interaction [48]. The 3D interaction of the miRNA with the mRNA was analyzed using molecular graphics tools like PyMol and Discovery Studio.

Molecular dynamics simulation (MD simulation). The MD simulation for nucleic acid is a very complex procedure. Compared to proteins, which usually have a globular structure, nucleic acids are extremely charged molecules, have a non-globular structure, and its stability is dependent entirely on the secondary structure [49, 50].

In this innovative study, we present the challenging MD simulation of the interaction between mRNA and microRNA. This groundbreaking approach allowed us to understand the dynamic binding and interaction of the two main players along with the stability of the complex, giving insights about their regulatory mechanisms.

The MD simulation was run as described in [51] using the NAMD package (version 2.14) for top five complexes obtained from the HDOCK results. For this, the system was prepared using the CHARMM36 force field with the HDOCK complexes as a starting point. By employing the Particle Mesh Ewald method, the electrostatic interactions were settled. The system was equilibrated for 2 ns, followed by a production phase for 50 ns, whereas the physiological environment was mimicked using the TIP3P model and neutralized using the appropriate ions Cl^- and Na^+. The simulation was run at 300K and a pressure of 1 atm in

an NPT ensemble (constant number of particles, pressure, and temperature). The edge effects were minimized by employing the periodic boundary conditions surrounding the mRNA-miRNA complex. VMD 1.9.3 software [38] was used for post-simulation analysis.

Expression analysis. The expression level of selected miRNAs was analyzed in the cell lines using miTED database [52]. The query was generated by providing the symbol of the selected miRNA, and the cell line option was selected for the search. The data was downloaded in a .tsv file, and expression in terms of reads per million (RPM) values of each miRNA was exported in a GraphPad Prism for graphical presentation.

Cell culture. Human breast cancer MCF-7 and melanoma ARN8 (parental A375) cells were cultured in Dulbecco's modified Eagle medium (DMEM) supplemented with 10% fetal bovine serum (FBS) (Life Technologies, USA), 100 units/mL penicillin, and 100 μg/mL streptomycin (Merck/Sigma-Aldrich, USA). The cells were cultured at 37 °C in humidified conditions with 5% CO_2.

miRNA inhibition. The lead miRNAs were inhibited in the MCF-7 cell line using the hairpin inhibitor of each miRNA purchased from Dharmacon, Horizon Discovery Limited (United Kingdom). The following inhibitors, called miRIDIAN, were used:

IH-302187-01-0002 as anti-*hsa-miR4651*, IH-300933-03-0002 as anti-*hsa-miR-608*, IH-302776-01-0002 as anti-*hsa-miR-6752-5p*, IH-302783-01-0002 as anti-*hsa-miR-6791-5p*, and IH-302800-01-0002 as anti-*hsa-miR-6796-5p.* D-001810-10-05 was used as a non-targeting control. Following the manufacturer' protocol, 12 nM of each RNA and DharmaFECT 1 Transfection Reagent (Cat No. T-2001-02) was used for transfection.

hTERT protein expression analysis. MCF-7 cells were seeded at a density of 60,000 cells per well in a 6-well plate and incubated overnight for adherence. On the following day, transfection with a hairpin inhibitor and control RNAs was performed, and the cells were incubated for 48 h. Then, cells were washed with phosphate buffered saline, and a Western blot analysis was performed. Briefly, whole-cell lysates were prepared using an RIPA lysis buffer containing protease inhibitor cocktail (Roche, Switzerland). 60 μg of protein from each sample was used. The samples were boiled in 1× Laemmli buffer at 95 °C for 10 min and separated by sodium dodecyl sulfate-polyacrylamide gel electrophoresis (SDS-PAGE) (NuPAGE™ Bis-Tris Mini Protein Gels, 10%, Invitrogen, USA). After gel electrophoresis, the separated proteins were transferred to the nitrocellulose membranes (Trans-Blot Turbo Transfer Pack, Cat No. 1704159, Bio-Rad, USA). The membranes were blocked with 5% non-fat milk (AppliChem GmbH, Germany) and probed with anti-hTERT primary antibody (Cat. No. AB32020-1001, Abcam Limited, United Kingdom) overnight at 4 °C. The horseradish peroxidase-tagged anti-mouse or anti-rabbit secondary antibodies (dilution 1:3000; Agilent Technologies, USA) were added followed by the incubation for 1 h and development using SuperSignal™ West Dura (Cat No. 34076, Thermo Fisher Scientific, USA). The immunoblots were imaged using a ChemiDoc XRS+ System (Bio-Rad, USA) and analyzed with the Image Lab software (Bio-Rad, USA). Beta-actin antibodies were used as loading controls. A PageRuler Plus Prestained protein ladder was used (Cat No. 26620, Thermo Fisher Scientific, USA). ImageLab software was used for quantification of each Western blot band. The mean volume of each band was considered. The fold-change of each sample to the β-actin mean volume was calculated. Using GraphPad Prism, the statistical significance was determined by the one-tailed non-parametric *t*-test between the control and the experimental sample; p-value < 0.05 was considered significant.

IncuCyte live-cell proliferation imaging. The MCF-7 and ARN8 cells were seeded in 96-well plates (1000 cells per well) in triplicate and treated with miRNAs. Cell proliferation was assessed by measuring confluence using the Incucyte® S3 Live-Cell imaging system (Sartorius, Germany). Four bright-field images per well were taken every 2 h for 3 days. Confluence was normalized versus the first time-point (0 h), For data analysis, Incucyte 2022B Rev2 software was used.

Results

Prediction of interaction sites between miRNAs and hTERT gene. The different insilico tools were used to predict the microRNA interaction sites on gene *hTERT*. The primary screening in the miRWalk database resulted in 3499 miRNA interactions with

hTERT. To filter out the worthy interactions, a stringent criterion was applied, where the interactions with the binding probability of 1 were considered, representing high-confidence interactions. Further, miRNAs with the binding energy ≤ –30 kcal/mol were filtered, showing a high binding affinity for *hTERT*. The interactions were further filtered by selecting those with an AU content of less than 0.6, which suggests a more stable and specific miRNA-mRNA interaction. Only 502 miRNA-mRNA interactions fulfilled these criteria.

To ensure the consistent prediction of miRNA binding sites on hTERT mRNA, the interactions identified in miRWalk were further validated by cross-checking in TargetScan and miRDB database. This scrutiny resulted in only 5 microRNAs (Table 1) that were common in the three databases and were constantly interacting with *hTERT* mRNA, representing high-confidence miRNAs for *hTERT* regulation.

Significant alignments between miRNAs and hTERT mRNA. To predict the potential binding sites, we used RNA22 software to align the selected miRNAs against *hTERT* mRNA (Ref: NM_001193376.3), consisting of 3850 nucleotides. RNA22 generated 110 miRNA-mRNA alignments where only 11 alignments showed statistical significance with a $p < 0.05$ (Table 2), representing strong and significant interactions. RNA22 generated results with an exact nucleotide position where miRNA binds to mRNA. It also calculates the folding energy (in kcal/mol) for each complex, representing the free energy or binding energy, which is crucial for assessing the strength and stability of the complex. More negative folding energy shows a stable and stronger binding energy, with a higher binding affinity.

RNA22 results showed that the strongest and energetically favorable interaction was shown by *hsa-miR-4651* with *hTERT,* interacting with the folding energy of —32kcal/mol, suggesting the potential regulatory role of *hsa-miR-4651* in *hTERT* expression.

Shortlisting of hTERT regions. The *hTERT* (Ref: NM_001193376.3) mRNA regions were shortlisted based on the interactions with the selected miRNAs. Briefly, RNA22 generated 110 hits of the miRNA-RNA clusters when we applied a threshold for a significant interaction at $p < 0.05$. As a result, six mRNA regions were selected for further analysis. Region 1 consisted of 140 nucleotides spanning 1—140 with seven interactions predicted by RNA22. Region 2 was divided into two parts because of its large size, recorded as region 2.1 and region 2.2, consisting of 318 and 313 nucleotides spanning the 1383—1700 and 1701—2013 regions, respectively, whereas the highest number of interactions were reported by RNA 22 with region 6, with 21 miRNA-mRNA interactions. The details of the selected regions are summarized in Table 3. These selected regions with high interaction miRNA frequency show areas with more potential in post-transcriptional *hTERT* regulation. The complete RNA22 result is provided in supplementary file 1.

Molecular docking analysis between miRNAs and hTERT. In RNA22 based analysis, we identified the important regions of *hTERT* mRNA from a regulatory point of view. Thus, we performed docking between these hotspot regions of *hTERT* mRNA and shortlisted miRNAs employing HDOCK. Each miRNA was docked with the six selected regions, giving off 35 complexes. The top complexes with stable orientation were selected with the maximum confidence score and minimum binding affinity, indicating the stable and best complex. The docking score reflects how strongly miRNA is attached to the mRNA, whereas the confidence score provides the reliability of the docking prediction.

The best interactions are summarized in Table 4 and depicted in Figs. 1—5. The docking analysis revealed that the miRNA *hsa-miR-4651* is the best docked with region 2:2 with a docking score of –374.35 and 0.988 confidence score. The top model obtained from HDOCK results showed that different mRNA residues from region 2.2 interacted with *hsa-miR-4651,* whereas the main residue in vicinity were ranging from mRNA nucleotides 120—130 of the region 2.2. The docking complex is visually represented in Fig. 1.

Furthermore, *hsa-miR-608* showed the best docking with region 3, with a docking score of –359.14 and a confidence score of 0.985. The best HDOCK model showed that a large loop of region 3 from the *hTERT* mRNA, including nucleotides 283—326, interacted with *hsa-miR-608* miRNA (Supplementary Fig. 1) [1].

[1] Supplementary materials are available at https://doi.org/10.5281/zenodo.16753638

Notably, both miRNA *hsa-miR-6796-5p* and *hsa-miR-6752-5p* exhibited the best docking results in region 4 with a docking score of –362.12 and –513.9 and confidence score of 0.985 and 0.999, respectively. Nucleotides 160—169 of mRNA region 4 were bonded with miRNA *hsa-miR-6796-5p* as shown in Fig. 2, whereas nucleotides 174—209 showed bonding with *hsa-miR-6752-5p* (Supplementary Fig. 2).

Table 1. **Top 5 shortlisted microRNAs with nucleotide sequence and length**

S. No.	microRNA	Sequence	Nucleotide length
1	*hsa-miR-6791-5p*	CCCCUGGGGCUGGGCAGGCGGA	22
2	*hsa-miR-6796-5p*	UUGUGGGGUUGGAGAGCUGGCUG	23
3	*hsa-miR-6752-5p*	GGGGGGUGUGGAGCCAGGGGGC	22
4	*hsa-miR-608*	AGGGGUGGUGUUGGGACAGCUCCGU	25
5	*hsa-miR-4651*	CGGGGUGGGUGAGGUCGGGC	20

Table 2. **RNA22 predicted alignments with $p < 0.05$**

S. No.	miRNA	Predicted target site (leftmost)	Folding energy (Kcal/mol)	Heteroduplex	*p*
1	*has-miR-6752_5p*	1432	–23.6	GCTCCGCCAGCACAGCAGCCCCT ||:|| | || | :|| ||||: CGGGG-GACCGAGGTGTGGGGGG	0.008
2	*hsa-miR-4651*	3318	–19.1	GC-AGACACCAGCAGCCCTG || ||| || | :|||:| CGGGCTGGAGTGGGTGGGGC	0.02
3	*hsa-miR-6752_5p*	2450	–18.4	GTCATCGAGCAGAGCTCCTCCC |:| | || :| ||:||| CGGGGGACCGAGGTGTGGGGGG	0.03
4	*hsa-miR-4651*	2450	–16.7	GTCATCGAGCAGAGCTCCTCCCTG |:| ||| | :| || |||:| CGG--GCTGG-AGTG-GGTGGGGC	0.03
5	*hsa-miR-6796_5p*	2873	–20.2	CAGACGGTGTGCACCAACATCTACAA ||| |:|: | |||| :|:|||| GTCGGTCG--AGAGGTTG-GGGTGTT	0.05
6	*hsa-miR-6752_5p*	3633	–27	CACCCCTCGC-CC-TGCCCTCC ||||| || || ::|||:|| CGGGGGACCGAGGTGTGGGGGG	0.05
7	*hsa-miR-608*	3641	–20.8	GCCCTGCCCTCCTTTGCCTTCCACCCCC || |||: :| |||||| TGCCTCGACAGGG-TTG—TGGTGGGGA	0.05
8	*hsa-miR-6796_5p*	54	–23.5	AAGCCCTGGCCCCGGCCACCCCCGCGA |||| :|| | ||| ||||:|: GTCGG--TCGAG—AGGTTGGGGTGTT	0.05
9	*hsa-miR-6752_5p*	54	–32	AAGCCCTGGCCCCGGCCACCCCCG |||||| ||: |||||| CGGGGGACCGAGGT—GTGGGGGG	0.05
10	*hsa-miR-608*	50	–25.7	TGGGAAGCCCTGGCCCCG--GC-CACCCCC ||| || || |||: :||||||| TGCCT-CG--AC-AGGGTTGTGGTGGGGA	0.05
11	*hsa-miR-4651*	56	–31.4	GCCCTGGCCCCGGCCACCCCC |||| |:|| |: ||||||| CGGG-CTGGAGTGGGTGGGGC	0.05

The docking results for *hsa-miR-6791-5p* showed a top docking complex with region 5 with a docking score of —451.35 and 0.9976 confidence score. The main residues of mRNA region 5 were ranging from 73—76 and 194—199 (Supplementary Fig. 3). Noteworthy, the root- mean-square distance of *hsa-miR-6791-5p* to region 5 was very low, which shows a stable interaction between these two moieties, demanding further analyses to explore the interaction.

MD Simulation. To further validate the stability of each miRNA-mRNA complex, we conducted MD simulation studies using the NAMD package. The MD simulation was extended over 50 ns to observe the binding dynamics and stability of each complex. The MD simulation analysis for region 4 vs *hsa-miR-6796-5p* showed that the complex has remained stable throughout the assigned duration. Consistent bonding and interactions were observed throughout the simulation run between mRNA and miRNA, contributing to the stability of the relevant complex. The miRNA maintained its position in the mRNA binding site without any observed deviation. The robustness of interaction can be visualized through Supplementary Movie SM1.

The MD simulation analysis of region 3 vs *hsa-miR-608* demonstrated consistent stability throughout the simulation. The key residues showed continuous bonding and interactions with the miRNA enforcing the stability of the complex. The visual demonstration of trajectory analysis is compiled in Supplementary Movie SM2, which illustrates that the miRNA is stably bounded to mRNA with no deviation observed throughout the simulation run. However, an unstable interaction was observed between region 4 of mRNA with *hsa-miR-6752-5p* miRNA. In the middle of the simulation run, the miRNA fully disassociated from the complex, suggesting a lack of strong molecular affinity between mRNA and miRNA in the simulation conditions (Supplementary Movie SM3). The trajectory analysis of region 2.2 with the *hsa-miR-4651* complex maintained structural integrity during MD simulation, with strong and stable interactions observed. The complex showed continuous engagement and consistent interactions between mRNA and miRNA throughout the MD simulation, with no worthy structural detachment (refer to Supplementary Movie SM4).

The pairing of mRNA region 5 with miRNA *hsa-miR-6791-5p* identifies high degree of stability with intact bonding and interactions observed between mRNA and miRNA nucleotides. The visual representation of trajectory analysis of MD simulation is compiled in Supplementary Movie SM5, showcasing strong and stable interaction within the complex with no drift observed during simulation run.

Expression of lead miRNA in cancer cells. The data from the miTED database showed that *hsa-miR-4651* and *hsa-miR-6796-5p* were highly expressed in cancer cells (Fig. 3). Importantly, the breast cancer cells MCF-7 and endometrial cancer HeLa cells were two cell lines that expressed all five identified miRNAs. Therefore, we selected MCF-7 cells as a model for in vitro analyses.

Table 3. ***hTERT*** **shortlisted regions**

S. No.	Name	Region	Number of nucleotides
1	Region 1	1—140	140
2	Region 2.1	1383—1700	318
3	Region 2.2	1701—2013	313
4	Region 3	2170—2520	351
5	Region 4	2813—3150	338
6	Region 5	3151—3360	210
7	Region 6	3501—3780	280

Table 4. **Shortlisted docked complexes from HDOCK**

S. No.	Complex	Docking Score	Confidence Score	Ligand rmsd (Å)
1	Region 4 vs *hsa-miR-6752_5p*	–513.96	0.9993	227.6
2	Region 5 vs *hsa-miR-6791-5p*	–451.35	0.9976	58.59
3	Region 2-2 vs *hsa-miR-4651*	–374.35	0.9889	129.91
4	Region 4 vs *hsa-miR-6796-5p*	–362.12	0.9858	109.35
5	Region 3 vs *hsa-miR-608*	–359.14	0.985	124.68

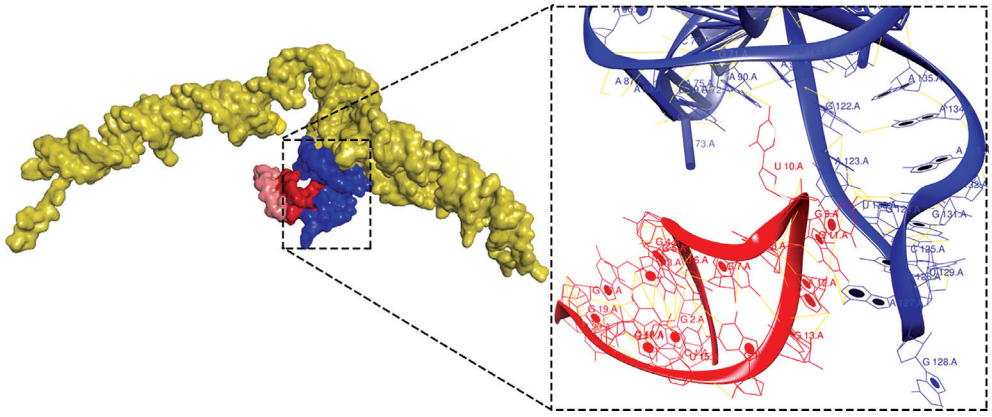

a *b*

Fig. 1. Interaction between mRNA Region 2.2 and hsa-miR-4651. *a* — Overview of the molecular interaction. The red region represents the binding site of microRNA, while the blue region corresponds to the binding site of mRNA. Unbound areas are depicted in pink for miRNA and yellow for mRNA. *b* — Close-up of docking results, highlighting specific nucleotide interactions. The blue mRNA nucleotides bind to the red microRNA nucleotides. The yellow dashed line indicates the bonding between the nucleotides

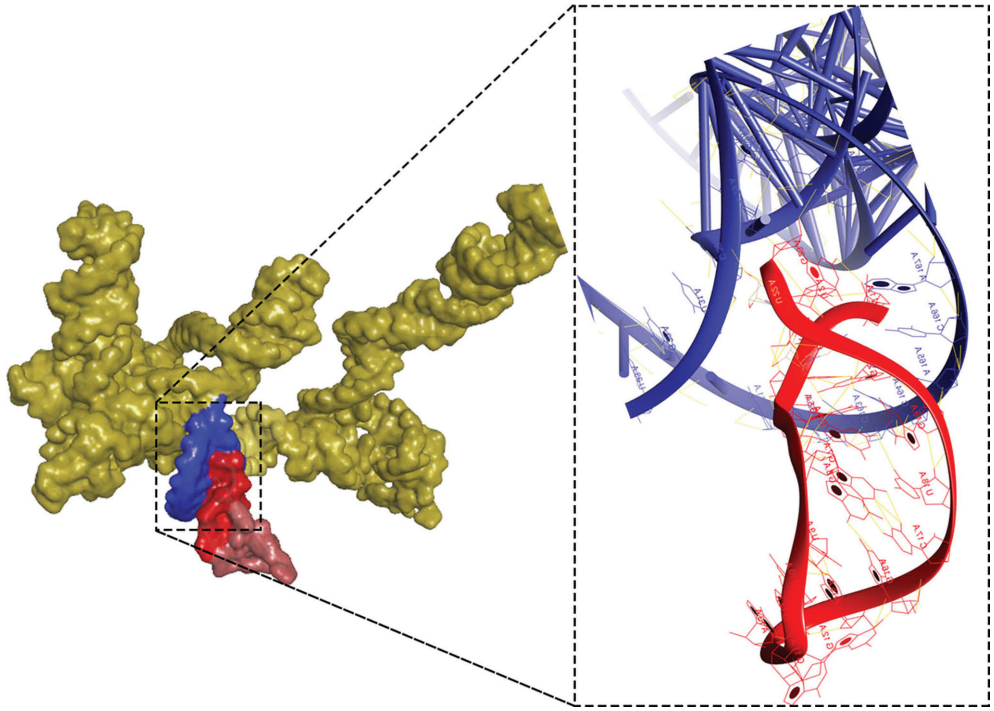

a *b*

Fig. 2. Interaction between mRNA Region 4 and hsa-miR-6796-5p. *a* — Overview of the molecular interaction. The red region indicates the microRNA binding site, while the blue region shows the mRNA binding site. Unbound areas are highlighted in pink for miRNA and yellow for mRNA. *b* — Detailed view of docking results, emphasizing nucleotide interactions. The blue mRNA nucleotides bind to red nucleotides of the microRNA, while the yellow dashed lines depict nucleotide bonding

Effect of miRNA inhibition on *hTERT* ***protein levels.*** Following the inhibition of the identified miRNAs, the protein expression of *hTERT* was evaluated in MCF-7 cells. Inhibition of *hsa-miR-6796-5p* led to a significant increase in the expression of *hTERT*. In contrast, inhibition of *hsa-miR-4651* significantly reduced the expression of the *hTERT* protein. There was no profound effect of *hsa-miR-6791-5p, hsa-miR-6752-5p,* and *hsa-miR-608* inhibition, as shown in Fig. 4, *a* and *b*.

Inhibition of selected miRNA and proliferation of cancer cells. The identified miRNAs were in-

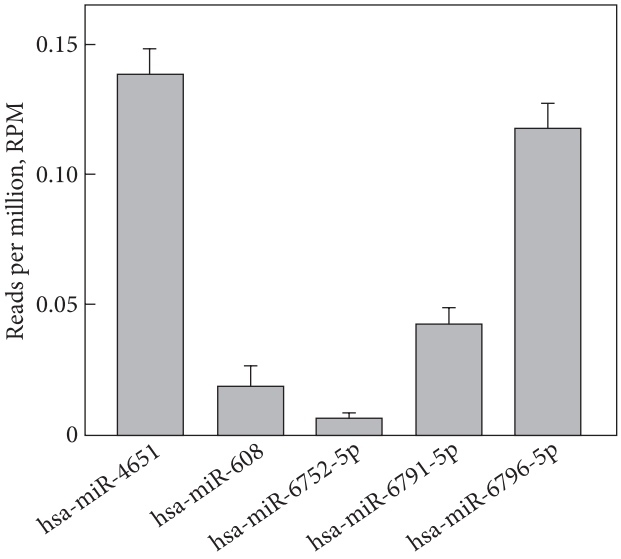

Fig. 3. Expression analysis of selected miRNAs. The data were retrieved from the miTED database for cell lines. Read per million (RPM) values were subjected to GraphPad Prism to generate the graph.

hibited in the breast cancer MCF-7 and melanoma ARN8 cells using commercial hairpin inhibitors by transfection. Cell proliferation was assessed by the live cell imaging using the Incucyte system, and the percent confluency was determined. The data showed that *hsa-miR-4651, hsa-miR-6791-5p,* and *hsa-miR-6752-5p* reduced the proliferation in both cell lines. There was no effect of *hsa-miR-6796-5p* and *hsa-miR-608* on the proliferation of these cells (Fig. 4 *c*, *d*).

Discussion

During carcinogenesis, telomerase can be activated by the expression of telomerase reverse transcriptase (TERT), which is a catalytic subunit of telomerase. The *hTERT* activation contributes to preserving the length of telomeres. Therefore, it maintains chromosomal stability and helps cells in avoiding senescence [53]. The telomere maintenance mechanisms (TMMs) were reported in 80% of tumors [54].

Most of the approaches for TERT regulation involve targeting at the transcriptional level [55]. The post-transcriptional regulation requires more research. Different miRNAs have been reported as TERT regulators. The miRNAs that downregulate TERT include *let-7g-3p, hsa-miR-133a, hsa-miR-1182, hsa-miR-128, miR-541-3p, hsa-miR-498,* and *miR-138-5p* [56]. In colorectal cancer, *miR-422a* and *miR-138-5p* have been shown to inhibit the TERT expression [57, 58]. *miR-138-5p* has also been shown to repress *hTERT* protein expression in cervical and thyroid carcinoma [56, 58]. Similarly, *miR-1207-5p, hsa-miR-1182, hsa-miR-532, hsa-miR-3064,* and *hsa-miR-1266* have been reported to bind with *hTERT* 3′UTR, thus repressing the growth and invasion of tumor in ovarian, bladder, and gastric cancer [54, 59]. In another study, miR-128 has been found to regulate the expression of TERT in teratoma and HeLa cells [60]. Finally, *hsa-miR-34a* acts as a tumor suppressor that induces cell senescence [61].

According to the study done on the expression profile of different miRNAs in breast cancer, *hsa-miR-6791-5p* was found to have clinical relevance. In particular, *hsa-miR-6791-5p* was upregulated in breast cancers, resulting in poor patient outcome and survival [62]. Another study conducted on breast cancer showed co-expression of phospholipase D3 (PLD3) and *hsa-miR-6796-5p* in the p53/ZEB1-PLD3 cycle regulating cell proliferation [63]. Previously, *hsa-miR-6796-5p* was linked with obesity as it regulates the lipid metabolism and insulin signaling [64]. *hsa-miR-608* is one of the newly discovered miRNAs, and its biological role is not yet fully described. According to study [57], *hsa-miR-608* may act as a tumor suppressor or oncomiR. In chordomas, which are rare malignant tumors, *hsa-miR-608* was found to play an active role as tumor suppressive miRNA, with *hsa-miR-608* levels being down regulated in the chordoma cell lines. In another study conducted using a qRT-PCR analysis, expression of *hsa-miR-608* was analyzed in glioblastoma, which is a highly lethal brain tumor. In this tumor, *hsa-miR-608* was found to be in glioma stem cells, which decreased its level and increased the pathological grade [65]. Using RT-qPCR, the decreased level of *hsa-miR-608* was also analyzed in AML patients [66]. Additional study showed an inverse relationship between *hsa-miR-608* overexpression and reduced expression of NAA10 mRNA and protein, thereby suppressing cell cycle progression, migration, and proliferation and tumorigenic capacity of cells [67].

Through the stringent in-silico analyses, we have identified 5 potential miRNAs as interactors of *hTERT* mRNA. Our expression analysis showed that most of the identified miRNAs are detectable

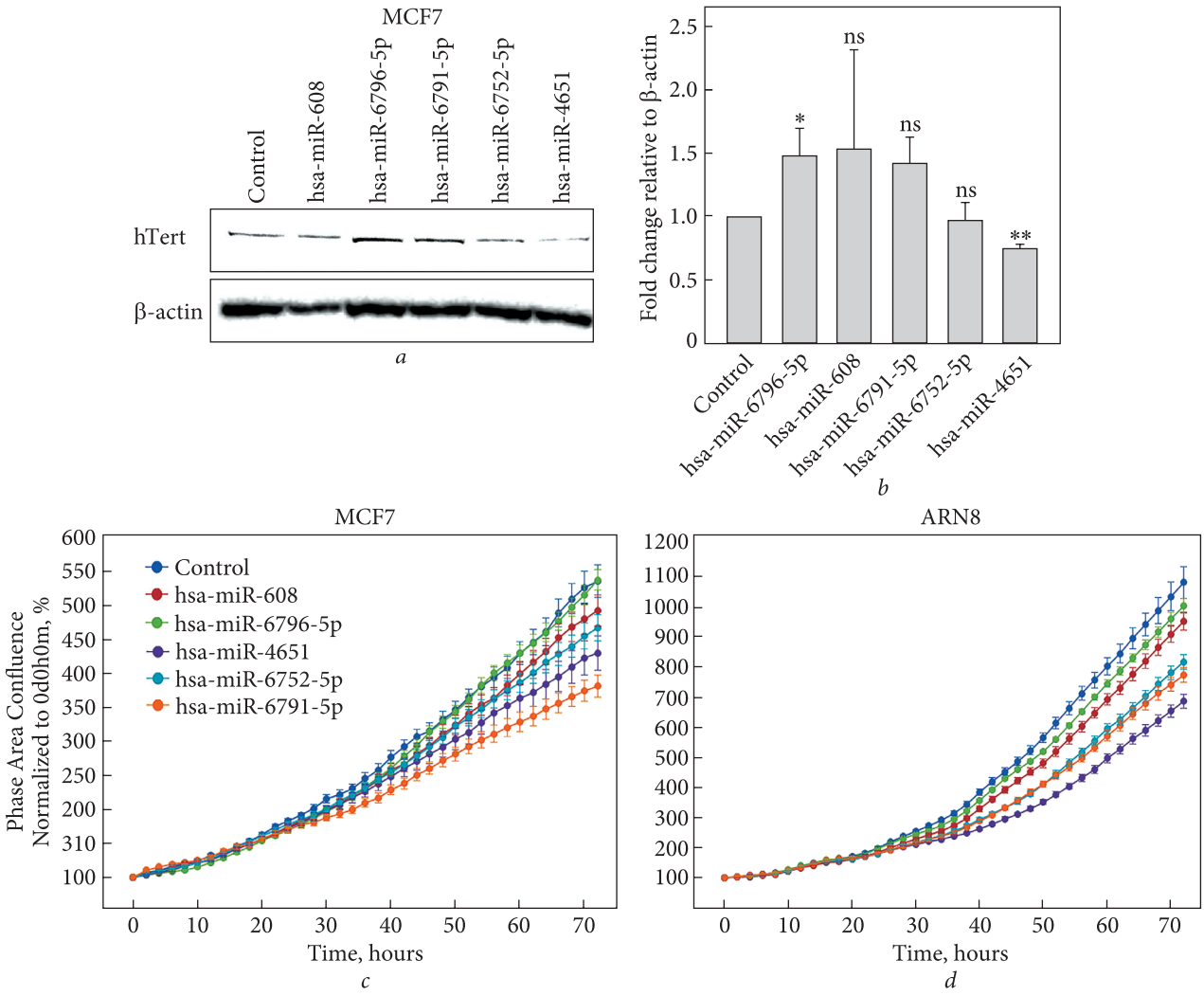

Fig. 4. Effect of lead miRNAs inhibition. MCF-7 cells were transfected using the commercial short hairpin inhibitor against each miRNA. *a* — Western blot analysis for hTERT protein expression level where β-actin was used as a loading control. *b* — Each band of blot in (*a*) was quantified and presented as graph fold change against control scrambled transfect cells. Statistical analysis: *t*-test with ns, * and ** indicate $p > 0.05$, $p < 0.05$, and $p < 0.01$, respectively. *c* — Effect of miRNA inhibition on proliferation of MCF-7 cells, after transfection with hairpin inhibitors confluency was measured by live cell imaging for 3 days in the IncuCyte system. Percent confluency normalized to time point 0 was calculated. *d* — Effect of inhibition of selected miRNA on the proliferation of melanoma ARN8 cells.

in HeLa and MCF-7 cells. In our study, the inhibition of *hsa-miR-6796-5p* in MCF-7 cells resulted in a significant increase in the expression of *hTERT* protein. In contrast, the inhibition of *hsa-miR-4651* in MCF-7 cells significantly reduced *hTERT* expression and cell proliferation. Further investigation is needed to confirm whether *hsa-miR-4651* acts as an oncomiR by directly enhancing the expression of *hTERT* or indirectly controls the expression of *hTERT* by regulating other factors that modulate the *hTERT* levels. The inhibition of *hsa-miR-6796-5p* did not affect the proliferation of cells, probably, because the cells were already in the maximum proliferative state and further increase in *hTERT* levels could not enhance the proliferation. Furthermore, the inhibition of *hsa-miR-6791-5p* also retarded the cell growth in an *hTERT*-independent manner as its inhibition did not alter the *hTERT* expression. No effect on the *hTERT* expression or cell proliferation was observed upon inhibition of *hsa-miR-608* and *hsa-miR-6752-5p*. Interestingly, we observed unstable interaction of *hsa-miR-6752-5p* with *hTERT* in our MD simulation analysis.

Our findings align with previous studies, which demonstrated miRNA-mediated *hTERT* regulation in colorectal cancer cells. This study provides a foun-

dation for future research into miRNA-based cancer therapies and highlights the need for additional experimental validation to ensure clinical applicability.

Acknowledgments

The authors express their sincere gratitude to Professor Sonia Lain from Karolinska Institute, Sweden, for her generosity in allowing us to conduct in vitro experiments and for reviewing the manuscript. The authors acknowledge the Theoretical and Computational Biophysics Group in the Beckman Institute for Advanced Science and Technology at the University of Illinois for NAMD. They also acknowledge with appreciation the access granted to HDOCK by Sheng-You Huang.

Funding

The study is financially supported by a grant from the BUITEMS Research Acceleration & Support (BRAS) Program, awarded to Dr. Muhammad Mushtaq Yasinzai.

Conflict of interest statement

The author(s) declare no potential conflicts of interest concerning the research, authorship, and/or publication of this article.

Availability of data and materials

All data generated or analyzed during this study are included in this article (including its Supplemental Files). Further details can be provided upon request to the corresponding author.

Supplementary Information

The supplementary data is available at:
https://doi.org/10.5281/zenodo.16753638

REFERENCES

1. Gillis AJ, Schuller AP, Skordalakes E. Structure of the Tribolium castaneum telomerase catalytic subunit TERT. *Nature*. 2008;455(7213):633-637. https://doi.org/10.1038/nature07283
2. Mitchell M, Gillis A, Futahashi M, et al. Structural basis for telomerase catalytic subunit TERT binding to RNA template and telomeric DNA. *Nat Struct Mol Biol*. 2010;17(4):513-518. https://doi.org/10.1038/nsmb.1777
3. Cong YS, Wen J, Bacchetti S. The human telomerase catalytic subunit hTERT: organization of the gene and characterization of the promoter. *Hum Mol Genet*. 1999;8(1):137-142. https://doi.org/10.1093/hmg/8.1.137
4. MacNeil DE, Bensoussan HJ, Autexier C. Telomerase regulation from beginning to the end. *Genes (Basel)*. 2016;7(9). https://doi.org/10.3390/genes7090064
5. Venteicher AS, Meng Z, Mason PJ, et al. Identification of ATPases pontin and reptin as telomerase components essential for holoenzyme assembly. *Cell*. 2008;132(6):945-957. https://doi.org/10.1016/j.cell.2008.01.019
6. Bryan TM, Reddel RR. Telomere dynamics and telomerase activity in in vitro immortalised human cells. *Eur J Cancer*. 1997;33(5):767-773. https://doi.org/10.1016/s0959-8049(97)00065-8
7. Lilleby W, Gaudernack G, Brunsvig PF, et al. Phase I/IIa clinical trial of a novel hTERT peptide vaccine in men with metastatic hormone-naive prostate cancer. *Cancer Immunol Immunother*. 2017;66(7):891-901. https://doi.org/10.1007/s00262-017-1994-y
8. Zanetti M. A second chance for telomerase reverse transcriptase in anticancer immunotherapy. *Nat Rev Clin Oncol*. 2017;14(2):115-128. https://doi.org/10.1038/nrclinonc.2016.67
9. Thompson PA, Drissi R, Muscal JA, et al. A phase I trial of imetelstat in children with refractory or recurrent solid tumors: a Children's Oncology Group Phase I Consortium Study (ADVL1112). *Clin Cancer Res*. 2013;19(23):6578-6584. https://doi.org/10.1158/1078-0432.Ccr-13-1117
10. Bryan C, Rice C, Hoffman H, et al. Structural basis of telomerase inhibition by the highly specific BIBR1532. *Structure*. 2015;23(10):1934-1942. https://doi.org/10.1016/j.str.2015.08.006
11. Biffi G, Tannahill D, McCafferty J, et al. Quantitative visualization of DNA G-quadruplex structures in human cells. *Nat Chem*. 2013;5(3):182-186. https://doi.org/10.1038/nchem.1548
12. Drosopoulos WC, Kosiyatrakul ST, Schildkraut CL. BLM helicase facilitates telomere replication during leading strand synthesis of telomeres. *J Cell Biol*. 2015;210(2):191-208. https://doi.org/10.1083/jcb.201410061
13. Tauchi T, Shin-ya K, Sashida G, et al. Telomerase inhibition with a novel G-quadruplex-interactive agent, telomestatin: in vitro and in vivo studies in acute leukemia. *Oncogene*. 2006;25(42):5719-5725. https://doi.org/10.1038/sj.onc.1209577
14. Liu W, Zhong YF, Liu LY, et al. Solution structures of multiple G-quadruplex complexes induced by a platinum(II)-based tripod reveal dynamic binding. *Nat Commun*. 2018;9(1):3496. https://doi.org/10.1038/s41467-018-05810-4
15. El-Daly H, Kull M, Zimmermann S, et al. Selective cytotoxicity and telomere damage in leukemia cells using the telomerase inhibitor BIBR1532. *Blood*. 2005;105(4):1742-1749. https://doi.org/10.1182/blood-2003-12-4322
16. Budakoti M, Panwar AS, Molpa D, et al. MicroRNA: The darkhorse of cancer. *Cell Signal*. 2021;83:109995. https://doi.org/10.1016/j.cellsig.2021.109995

17. Smolarz B, Durczyński A, Romanowicz H, et al. miRNAs in cancer (review of literature). *Int J Mol Sci*. 2022;23(5):2805. https://doi.org/10.3390/ijms23052805
18. Hussen BM, Hidayat HJ, Salihi A, et al. MicroRNA: A signature for cancer progression. *Biomed Pharmacother*. 2021;138:111528. https://doi.org/10.1016/j.biopha.2021.111528
19. Peng Y, Croce CM. The role of microRNAs in human cancer. *Signal Transduct Target Ther*. 2016;1:15004. https://doi.org/10.1038/sigtrans.2015.4
20. Yi M, Xu L, Jiao Y, et al. The role of cancer-derived microRNAs in cancer immune escape. *J Hematol Oncol*. 2020;13(1):25. https://doi.org/10.1186/s13045-020-00848-8
21. Otmani K, Rouas R, Lewalle P. OncomiRs as noncoding RNAs having functions in cancer: Their role in immune suppression and clinical implications. *Front Immunol*. 2022;13:913951. https://doi.org/10.3389/fimmu.2022.913951
22. Hrdličková R, Nehyba J, Bargmann W, et al. Multiple tumor suppressor microRNAs regulate telomerase and TCF7, an important transcriptional regulator of the Wnt pathway. *PLoS One*. 2014;9(2):e86990. https://doi.org/10.1371/journal.pone.0086990
23. Cho WC. OncomiRs: the discovery and progress of microRNAs in cancers. *Mol Cancer*. 2007;6:60. https://doi.org/10.1186/1476-4598-6-60
24. Bai L, Wang H, Wang AH, et al. MicroRNA-532 and microRNA-3064 inhibit cell proliferation and invasion by acting as direct regulators of human telomerase reverse transcriptase in ovarian cancer. *PLoS One*. 2017;12(3):e0173912. https://doi.org/10.1371/journal.pone.0173912
25. Li J, Lei H, Xu Y, et al. miR-512-5p suppresses tumor growth by targeting hTERT in telomerase positive head and neck squamous cell carcinoma in vitro and in vivo. *PLoS One*. 2015;10(8):e0135265. https://doi.org/10.1371/journal.pone.0135265
26. Zhou J, Dai W, Song J. miR-1182 inhibits growth and mediates the chemosensitivity of bladder cancer by targeting hTERT. *Biochem Biophys Res Commun*. 2016;470(2):445-452. https://doi.org/10.1016/j.bbrc.2016.01.014
27. Chen L, Lü MH, Zhang D, et al. miR-1207-5p and miR-1266 suppress gastric cancer growth and invasion by targeting telomerase reverse transcriptase. *Cell Death Dis*. 2014;5(1):e1034. https://doi.org/10.1038/cddis.2013.553
28. Mitomo S, Maesawa C, Ogasawara S, et al. Downregulation of miR-138 is associated with overexpression of human telomerase reverse transcriptase protein in human anaplastic thyroid carcinoma cell lines. *Cancer Sci*. 2008;99(2):280-286. https://doi.org/10.1111/j.1349-7006.2007.00666.x
29. Cittelly DM, Das PM, Spoelstra NS, et al. Downregulation of miR-342 is associated with tamoxifen resistant breast tumors. *Mol Cancer*. 2010;9:317. https://doi.org/10.1186/1476-4598-9-317
30. Lewis KA, Tollefsbol TO. Regulation of the telomerase reverse transcriptase subunit through epigenetic mechanisms. *Front Genet*. 2016;7:83. https://doi.org/10.3389/fgene.2016.00083
31. Liu K, Li L, Rusidanmu A, et al. Down-regulation of miR-1294 is related to dismal prognosis of patients with esophageal squamous cell carcinoma through elevating c-myc expression. *Cell Physiol Biochem*. 2015;36(1):100-110. https://doi.org/10.1159/000374056
32. Östling P, Leivonen SK, Aakula A, et al. Systematic analysis of microRNAs targeting the androgen receptor in prostate cancer cells. *Cancer Res*. 2011;71(5):1956-1967. https://doi.org/10.1158/0008-5472.Can-10-2421
33. Xu X, Chen W, Miao R, et al. miR-34a induces cellular senescence via modulation of telomerase activity in human hepatocellular carcinoma by targeting FoxM1/c-Myc pathway. *Oncotarget*. 2015;6(6):3988-4004. https://doi.org/10.18632/oncotarget.2905
34. Sticht C, De La Torre C, Parveen A, et al. miRWalk: An online resource for prediction of microRNA binding sites. *PLoS One*. 2018;13(10):e0206239. https://doi.org/10.1371/journal.pone.0206239
35. Agarwal V, Bell GW, Nam J-W, et al. Predicting effective microRNA target sites in mammalian mRNAs. *eLife*. 2015;4:e05005. https://doi.org/10.7554/eLife.05005
36. McGeary SE, Lin KS, Shi CY, et al. The biochemical basis of microRNA targeting efficacy. *Science*. 2019;366(6472). https://doi.org/10.1126/science.aav1741
37. Chen Y, Wang X. miRDB: an online database for prediction of functional microRNA targets. *Nucleic Acids Res*. 2020;48(D1):D127-D131. https://doi.org/10.1093/nar/gkz757
38. Li D, Knox B, Gong B, et al. Identification of translational microRNA biomarker candidates for ketoconazole-induced liver injury using next-generation sequencing. *Toxicol Sci*. 2021;179(1):31-43. https://doi.org/10.1093/toxsci/kfaa162
39. Miranda KC, Huynh T, Tay Y, et al. A pattern-based method for the identification of microRNA binding sites and their corresponding heteroduplexes. *Cell*. 2006;126(6):1203-1217. https://doi.org/10.1016/j.cell.2006.07.031
40. Miranda KC, Huynh T, Tay Y, et al. A pattern-based method for the identification of MicroRNA binding sites and their corresponding heteroduplexes. *Cell*. 2006;126(6):1203-1217. https://doi.org/10.1016/j.cell.2006.07.031
41. Hassan M, Iqbal MS, Naqvi S, et al. Prediction of site directed miRNAs as key players of Transcriptional regulators against influenza C virus infection through computational approaches. *Front Mol Biosci*. 2022;9:866072. https://doi.org/10.3389/fmolb.2022.866072
42. Sayers EW, Bolton EE, Brister JR, et al. Database resources of the national center for biotechnology information. *Nucleic Acids Res*. 2022;50(D1):D20-D26. https://doi.org/10.1093/nar/gkab1112

43. Kozomara A, Birgaoanu M, Griffiths-Jones S. miRBase: from microRNA sequences to function. *Nucleic Acids Res*. 2019;47(D1):D155-D162. https://doi.org/10.1093/nar/gky1141
44. Sarzynska J, Popenda M, Antczak M, et al. RNA tertiary structure prediction using RNAComposer in CASP15. *Proteins*. 2023;91(12):1790-1799. https://doi.org/10.1002/prot.26578
45. Antczak M, Popenda M, Zok T, et al. New functionality of RNAComposer: an application to shape the axis of miR160 precursor structure. *Acta Biochim Pol*. 2016;63(4):737-744. https://doi.org/10.18388/abp.2016_1329
46. Parisien M, Major F. The MC-Fold and MC-Sym pipeline infers RNA structure from sequence data. *Nature*. 2008;452(7183):51-55. https://doi.org/10.1038/nature06684
47. Yao J, Reinharz V, Major F, et al. RNA-MoIP: prediction of RNA secondary structure and local 3D motifs from sequence data. *Nucleic Acids Res*. 2017;45(W1):W440-W444. https://doi.org/10.1093/nar/gkx429
48. Yan Y, Tao H, He J, et al. The HDOCK server for integrated protein-protein docking. *Nat Protoc*. 2020;15(5):1829-1852. https://doi.org/10.1038/s41596-020-0312-x
49. Cheatham TE, 3rd. Simulation and modeling of nucleic acid structure, dynamics and interactions. *Curr Opin Struct Biol*. 2004;14(3):360-367. https://doi.org/10.1016/j.sbi.2004.05.001
50. Mackerell AD, Jr., Nilsson L. Molecular dynamics simulations of nucleic acid-protein complexes. *Curr Opin Struct Biol*. 2008;18(2):194-199. https://doi.org/10.1016/j.sbi.2007.12.012
51. Shah K, Ansari M, Saeed S, et al. Nilotinib: disrupting the MYC-MAX heterocomplex. *Bioinform Biol Insights*. 2024;18:11779322241267056. https://doi.org/10.1177/11779322241267056
52. Kavakiotis I, Alexiou A, Tastsoglou S, et al. DIANA-miTED: a microRNA tissue expression database. *Nucleic Acids Research*. 2021;50(D1):D1055-D1061. https://doi.org/10.1093/nar/gkab733
53. Daniel M, Peek GW, Tollefsbol TO. Regulation of the human catalytic subunit of telomerase (hTERT). *Gene*. 2012;498(2):135-146. https://doi.org/10.1016/j.gene.2012.01.095
54. Gaspar TB, Sá A, Lopes JM, et al. Telomere maintenance mechanisms in cancer. *Genes (Basel)*. 2018;9(5):241. https://doi.org/10.3390/genes9050241
55. Dratwa M, Wysoczańska B, Łacina P, et al. TERT-regulation and roles in cancer formation. *Front Immunol*. 2020;11:589929. https://doi.org/10.3389/fimmu.2020.589929
56. Schrank Z, Khan N, Osude C, et al. Oligonucleotides targeting telomeres and telomerase in cancer. *Molecules*. 2018;23(9):2267. https://doi.org/10.3390/molecules23092267
57. Zhang Y, Schiff D, Park D, et al. MicroRNA-608 and microRNA-34a regulate chordoma malignancy by targeting EGFR, Bcl-xL and MET. *PLoS One*. 2014;9(3):e91546. https://doi.org/10.1371/journal.pone.0091546
58. Chai L, Kang XJ, Sun ZZ, et al. MiR-497-5p, miR-195-5p and miR-455-3p function as tumor suppressors by targeting hTERT in melanoma A375 cells. *Cancer Manag Res*. 2018;10:989-1003. https://doi.org/10.2147/cmar.S163335
59. Cukusić A, Skrobot Vidacek N, Sopta M, et al. Telomerase regulation at the crossroads of cell fate. *Cytogenet Genome Res*. 2008;122(3-4):263-272. https://doi.org/10.1159/000167812
60. Guzman H, Sanders K, Idica A, et al. miR-128 inhibits telomerase activity by targeting TERT mRNA. *Oncotarget*. 2018;9(17):13244-13253. https://doi.org/10.18632/oncotarget.24284
61. Leão R, Apolónio JD, Lee D, et al. Mechanisms of human telomerase reverse transcriptase (hTERT) regulation: clinical impacts in cancer. *J Biomed Sci*. 2018;25(1):22. https://doi.org/10.1186/s12929-018-0422-8
62. Prajapati KS, Shuaib M, Kushwaha PP, et al. Identification of cancer stemness related miRNA(s) using integrated bioinformatics analysis and in vitro validation. *3 Biotech*. 2021;11(10):446.https://doi.org/10.1007/s13205-021-02994-3
63. Liu BW, Sun N, Lin H, et al. The p53/ZEB1-PLD3 feedback loop regulates cell proliferation in breast cancer. *Cell Death Dis*. 2023;14(11):751. https://doi.org/10.1038/s41419-023-06271-4
64. Rovira-Llopis S, Díaz-Rúa R, Grau-Del Valle C, et al. Characterization of differentially expressed circulating miRNAs in metabolically healthy versus unhealthy obesity. *Biomedicines*. 2021;9(3):321. https://doi.org/10.3390/biomedicines9030321
65. Wang XB, Tian XY, Li Y, et al. Elevated expression of macrophage migration inhibitory factor correlates with tumor recurrence and poor prognosis of patients with gliomas. *J Neurooncol*. 2012;106(1):43-51. https://doi.org/10.1007/s11060-011-0640-3
66. Zuo W, Zhou K, Deng M, et al. LINC00963 facilitates acute myeloid leukemia development by modulating miR-608/MMP-15. *Aging (Albany NY)*. 2020;12(19):18970-18981. https://doi.org/10.18632/aging.103252
67. Yang H, Li Q, Niu J, et al. microRNA-342-5p and miR-608 inhibit colon cancer tumorigenesis by targeting NAA10. *Oncotarget*. 2016;7(3):2709-2720. https://doi.org/10.18632/oncotarget.6458

Submitted: July 01, 2025

Махам Ансарі, Рафіулла Рафіулла,
Абдул Валі, Афрасіаб Хан Тарін, Імрана
Ніяз Султан, Мухаммад Муштаг Ясінзай

Кафедра біотехнології, факультет наук про життя та інформатики,
Белуджистанський університет інформаційних технологій,
інженерії та управлінських наук (BUITEMS), Кветта, Пакистан

ІДЕНТИФІКАЦІЯ ТА ФУНКЦІОНАЛЬНА ХАРАКТЕРИСТИКА МІКРОРНК, ЩО РЕГУЛЮЮТЬ hTERT

Стан питання. Теломераза — це зворотна транскриптаза, яка реплікує кінці хромосом, тим самим підтримуючи цілісність геному. Її інгібування може сприяти запобіганню злоякісній трансформації клітин. Для таргетного впливу на *hTERT* застосовувалися різні підходи, і однією з перспективних стратегій є використання мікроРНК (міРНК). **Мета роботи** полягала у дослідженні взаємодії мікроРНК з *hTERT* із урахуванням афінності та оптимальної конформації взаємодії, а також вивченні впливу мікроРНК на експресію *hTERT* in vitro. Матеріали та методи. Для скринінгу використовувалися бази даних miRWalk, TargetScan та miRDB. У всіх трьох базах даних було виявлено п'ять мікроРНК з найвищим ступенем хітування, які могли взаємодіяти з мРНК *hTERT*, а саме hsa-miR-4651, hsa-miR-608, hsa-miR-6796-5p, hsa-miR-6752-5p та hsa-miR-6791-5p. Застосовували алгоритми та інструменти in silico, щоб змоделювати структури взаємодіючої мікроРНК та мРНК *hTERT*. Потім було проведено докінг і проаналізовано стабільність комплексів мікроРНК-мРНК за допомоги молекулярно-динамічної симуляції. **Результати.** Експресія вибраних мікроРНК була пригнічена в лінії клітин раку молочної залози MCF-7. Пригнічення hsa-miR-6796-5p посилювало, тоді як hsa-miR-4651 значно знижувало експресію білка *hTERT*. Більше того, пригнічення експресії hsa-miR-4651 привело до зниження швидкості проліферації клітин меланоми та раку молочної залози. **Висновки.** Запропоновано детальну процедуру ідентифікації та перевірки мікроРНК відносно їх взаємодії з мРНК. Пригнічення певних мікроРНК може модулювати експресію *hTERT* та впливати таким чином на проліферацію клітин, що може бути одним з підходів для цільової терапії раку. Ця стратегія може бути застосована і до інших генів з метою скринінгу потенційних мікроРНК, які впливають на експресію відповідних мРНК.

Ключові слова: мікроРНК, *hTERT*, злоякісні новоутворення, hsa-miR-6796-5p, hsa-miR-4651, орієнтація зв'язування, афінність, проліферація клітин.